

# Atomistic study of the anisotropic interaction between extended and point defects in crystalline silicon and its influence on Si self-interstitial diffusion

I. Santos,\* M. Aboy, L. A. Marqués, P. López,  
M. Ruiz, L. Pelaz

Departamento de Electricidad y Electrónica  
Universidad de Valladolid, Valladolid, Spain

\*corresponding author: [ivasan@tel.uva.es](mailto:ivasan@tel.uva.es)

A. M. Hernández-Díaz, P. Castrillo  
Departamento de Ciencias Politécnicas  
UCAM, Universidad Católica de Murcia,  
Murcia, Spain

**Abstract**—In this work we propose a methodology to analyze the elastic energy interaction at the atomic level between Si self-interstitials and extended defects in crystalline Si. The representation of this energy in maps in 2D planes shows the anisotropic nature of the elastic interaction. This elastic energy maps can be used to understand diffusion trajectories of Si self-interstitials around extended defects obtained from classical molecular dynamics simulations. The combined analysis of these trajectories and the elastic energy maps shows preferential capture directions around extended defects.

**Keywords**—Atomistic simulations, strain fields, elastic interaction, point defects, extended defects, crystalline silicon

## I. INTRODUCTION

The presence of defects in the semiconductor lattice highly influence the final device characteristics [1]. In order to prevent the negative effects that defects can induce or enhance the positive ones, accurate and physically based models are required to describe how defects diffuse and interact during semiconductor processing [2, 3]. Defect and dopant migration and interaction in Si is known to be affected by the presence of strain fields [4, 5, 6]. Nevertheless, existing models for defect evolution only take into account strain fields due to external factors, such as the biaxial strain in the channel of MOSFET devices or the build-in strain in lattice mismatched heterostructures. However, defects themselves create strain fields in their surroundings that can affect the evolution of other defects during annealing treatments [7].

In this work we analyze the elastic energy interaction among Si self-interstitials and extended defects. We focus this manuscript on the {311} defects, but the procedure is transferable to other extended defects such as (100) loops or (111) loops. We correlate the energy with the diffusion trajectories of the Si self-interstitial around the extended defects to evaluate the preferential capture directions.

## II. METHOD

We have developed a model that provides the elastic energy of the interaction between point defects and extended

defects in crystalline materials. The main hypothesis of the method is that the point defect introduces a small perturbation on the strain/stress field generated by an extended defect. Then, we decomposed the elastic interaction in two parts: the background field generated by the extended defect and the perturbation field induced by the point defect. This decomposition also affects components of the strain and stress tensorial fields:

$$\sigma_{ij} = \sigma_{ij}^B + \sigma_{ij}^d \quad \varepsilon_{ij} = \varepsilon_{ij}^B + \varepsilon_{ij}^d \quad (1)$$

where  $\sigma$  represents the stress field,  $\varepsilon$  the strain field, and superscripts  $B$  and  $d$  refers to background and defect fields, respectively. We evaluate the energy of the elastic interaction ( $E_{elastic}$ ) between the extended defect and the point defect in a certain position using this expression that has been particularized for cubic systems:

$$E_{elastic} = (\sigma_{11}\varepsilon_{11} + \sigma_{22}\varepsilon_{22} + \sigma_{33}\varepsilon_{33} + 2\sigma_{12}\varepsilon_{12} + 2\sigma_{13}\varepsilon_{13} + 2\sigma_{23}\varepsilon_{23})/2 \quad (2)$$

In our model we consider the value of the strain and stress fields at the atomic positions, and  $E_{elastic}$  is evaluated by a summation over all the atomic positions in the simulation cell. These values are obtained from conjugate gradient relaxations of defect configurations using the code LAMMPS [8]. We have chosen the Tersoff empirical potential within its third parametrization [9] to describe the Si-Si interactions. This empirical potential correctly describes structures different from perfect crystal, as it is the case of intrinsic defects and the amorphous phase [10, 11, 12, 13]. In particular, it provides an adequate description of {311} extended defects [12] and (100) and (111) loops in Si [13]. The energy of the elastic interaction between a point defect in a given position and an extended defect is evaluated from (2) taking into account the decomposition of stress and strain fields of (1). This procedure allows us easily reducing the tensorial elastic interaction between extended and point defects a scalar physically significant magnitude, i.e. the elastic energy. Moving the point defect around the extended defect and using (2) at every position, allows us mapping the elastic interaction energy map around the extended defect.

## III. RESULTS

We have represented in Fig. 1 the energy map of the elastic interaction of the Si self-interstitial and a  $\{311\}$  defect, a (100) loop, and a (111) loop. This representation highlights the anisotropic nature of the interaction. Regions with positive elastic energy interaction appear along the  $[311]$  direction for the  $\{311\}$  defect, along the  $[001]$  for the (100) loop, and along the  $[111]$  direction for the (111) loop. These direction corresponds to the regions over and below the characteristic planes of the defects. On the other hand, negative energies dominate in the characteristic plane of the defects. For distances far away the defects the elastic energy is negligible, as it is expected.

We performed classical molecular dynamic simulations with Tersoff potential of Si self-interstitial diffusion in the vicinity of the defects in order to correlate its trajectory with the obtained anisotropic elastic energy map. For this purpose, we place a Si self-interstitial at different positions around the defects, and we followed its trajectory during the simulation. We represent in the left part of Fig. 2 the obtained trajectory for a Si self-interstitial placed at  $(40 \text{ \AA}, 0, 0)$  on the side of the  $\{311\}$  defect, together with the elastic energy map previously evaluated. The defect perform some random hops initially, but as it enters the region with more negative elastic energies, it moves directly to the  $\{311\}$  defect. During its movement, the y and z coordinates does not change too much, which means that the defect moves approximately in the same XY plane.

For a better correlation between the trajectory and the elastic energy map, we represent in the right part of Fig. 2

the elastic energy associated to the position of the self-interstitial as a function of the X coordinate for different initial positions. It can be see that the elastic energy is reduced as the interstitial approaches the  $\{311\}$  defect. For distances larger than  $30 \text{ \AA}$  the interstitial moves with random hops due to the small variation produced in the elastic energy. However, for distances smaller than  $20 \text{ \AA}$ , the movement is directed towards the  $\{311\}$  defect.

We also analyzed the case in which the Si self-interstitial is initially placed in a region with positive elastic energy. We represent in the left part of Fig. 3 the resulting trajectory of a self-interstitial placed at  $(10 \text{ \AA}, -20 \text{ \AA}, 20 \text{ \AA})$  from the center of mass of the  $\{311\}$  defect, together with the elastic energy map. In this case, the trajectory of the defect is more complex, and all its coordinates change. Nevertheless, it can be seen that the defect is initially directed away far from the  $\{311\}$  defect. For a better analysis of the trajectory, we represent in the left side of Fig. 3 the elastic energy associated to the position of the self-interstitial as a function of its X coordinate. The initial trend shows that as the self-interstitial moves away the vicinity of the  $\{311\}$  defect, the elastic energy is reduced. Then the self-interstitial reaches a region with negligible elastic energies, and the movement turns random. The self-interstitial eventually tends to move towards regions with negative elastic energies.

Although we have only presented here the dynamics of the Si self-interstitial around the  $\{311\}$  defect, equivalent results are obtained for the (100) and (111) loops.

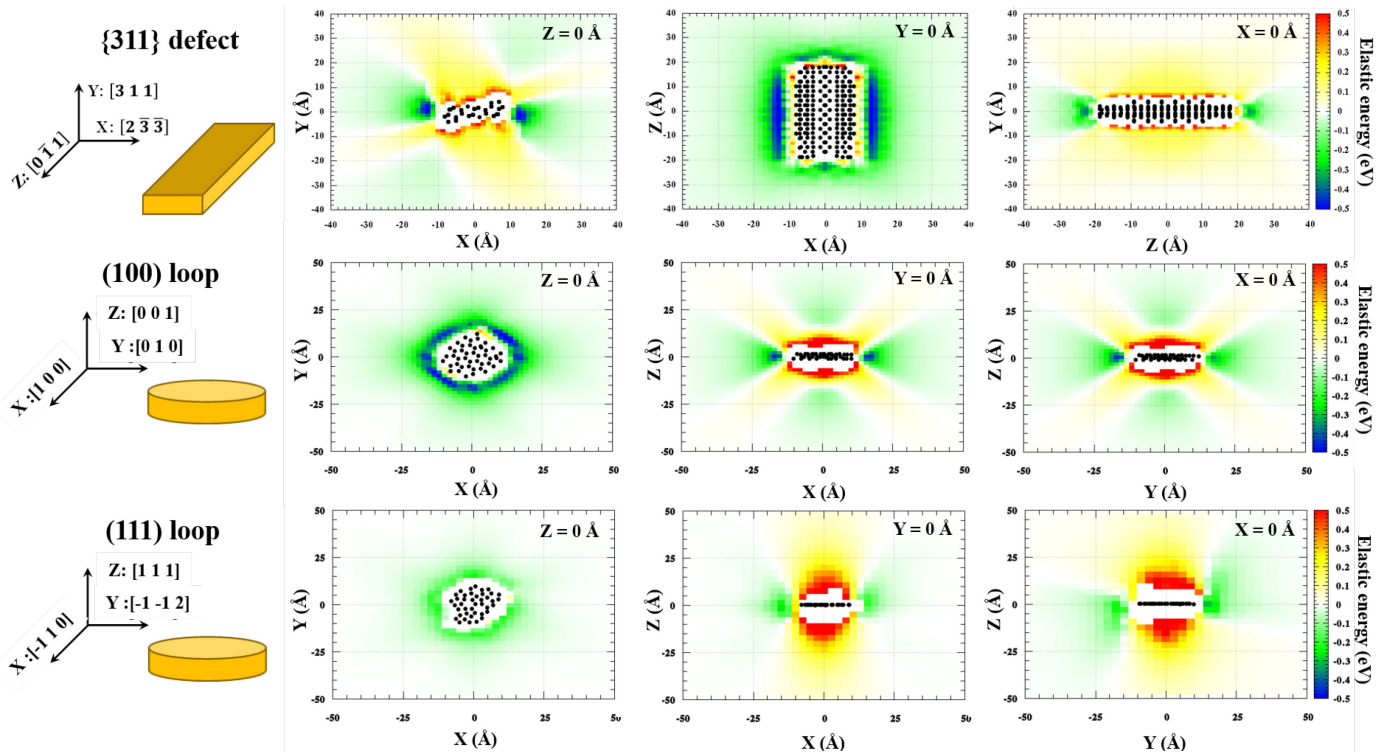


Fig. 1. Energy maps of the elastic interaction of the Si self-interstitial and a  $\{311\}$  defect, a (100) loop, and a (111) loop. Maps are shown at the principal planes of the defects, and the representations are centered at the center of mass of the defects. Schematics on the left show the crystallographic orientations of principal directions. Black dots in energy maps represent the displaced atoms that belong to the extended defects, while atoms at the perfect lattice are not shown.

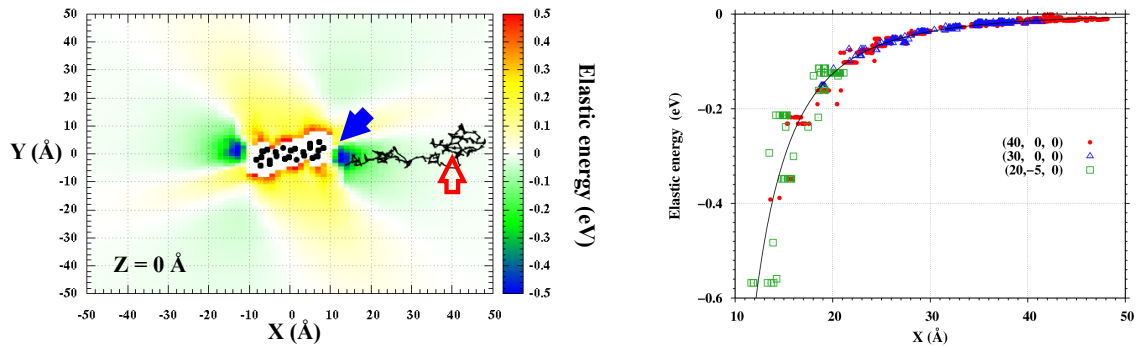


Fig. 2. (left) Si self-interstitial diffusion trajectory approaching the  $\{311\}$  defect in the direction  $[X,0,0]$  along with the corresponding elastic energy map. The empty red arrow indicates the initial position of the Si self-interstitial at  $(40 \text{ \AA}, 0, 0)$ , and the solid blue arrow indicates the capture point. (right) Correlation between the position of the the Si self-interstitial and the corresponding elastic energy at this position for different initial positions around the  $\{311\}$  defect. Solid line is to guide the eye.

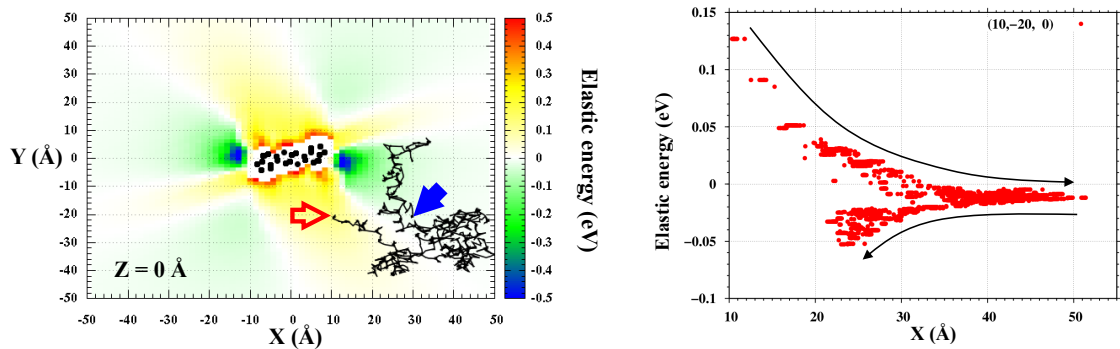


Fig. 3. (left) Si self-interstitial diffusion trajectory moving away the  $\{311\}$  defect along with the corresponding elastic energy map. The empty red arrow indicates the initial position of the Si self-interstitial at  $(10 \text{ \AA}, -20 \text{ \AA}, 20 \text{ \AA})$ , and the solid arrow indicates the final position. (right) Correlation between the position of the Si self-interstitial and the corresponding elastic energy. Black arrows indicate the evolution of the elastic energy with the Si self-interstitial motion.

#### IV. CONCLUSIONS

We quantified the elastic interaction between extended and point defects from the decomposition of the total field in a background field generated by the extended defect and a perturbation field induced by the point defect. We found from the representation of the elastic energy in 2D maps that the elastic interaction is highly anisotropic. The obtained elastic energy maps helped to explain the dynamics of Si self-interstitials around extended defects: they move towards regions that reduce the interacting elastic energy. This results in preferential capture directions around the extended defects.

#### ACKNOWLEDGMENT

This work has been funded by the Spanish Government under project TEC2014-60694-P, and the JCYL Consejería de Educación y Cultura under project VA331U14.

#### REFERENCES

[1] International Technology Roadmap for Semiconductors. See <http://www.itrs.net/>  
 [2] L. Pelaz, L. A. Marqués, M. Aboy, P. López, and I. Santos, "Front-end process modeling in silicon", *Eur. Phys. J. B* 72, 323 (2009)  
 [3] M. Aboy, I. Santos, L. Pelaz, L. A. Marqués, P. López, "Modeling of defects, dopant diffusion and clustering in silicon", *J Comput Electron* 13, 40 (2014)

[4] M. J. Aziz, "Stress effects on defects and dopant diffusion in Si", *Materials Science in Semiconductor Processing* 4, 397 (2001)  
 [5] K. Sueoka, E. Kamiyama, and J. Vanhellemont, "Theoretical study of the impact of stress on the behavior of intrinsic point defects in large-diameter defect-free Si crystals", *J. Cryst. Growth* 363, 97 (2013)  
 [6] M. J. Aziz, Y. Zhao, H.-J. Gossmann, S. Mitha, S. P. Smith, D. Schiferl, "Pressure and stress effects on the diffusion of B and Sb in Si and Si-Ge alloys", *Phys. Rev. B* 76, 054101 (2006)  
 [7] T. Isoda, M. Uematsu, K. M. Itoh, "Observation of silicon self-diffusion enhanced by the strain originated from end-of-range defects using isotope multilayers", *J. Appl. Phys.* 118, 115706 (2015)  
 [8] S. Plimpton, "Fast Parallel Algorithms for Short-Range Molecular Dynamics", *J Comp Phys*, 117, 1-19 (1995), <http://lammps.sandia.gov/>  
 [9] J. Tersoff, "Empirical interatomic potential for silicon with improved elastic properties", *Phys. Rev. B* 38, 9902 (1988)  
 [10] L. A. Marqués, L. Pelaz, M. Aboy, J. Barbolla, "The laser annealing induced phase transition in silicon: a molecular dynamics study". *Nucl. Instrum. Methods Phys. Res. B* 216, 57 (2004)  
 [11] L. A. Marqués, L. Pelaz, P. Castrillo and J. Barbolla, "Molecular dynamics study of the configurational and energetic properties of the silicon self-interstitial", *Phys. Rev. B* 71, 085204 (2005)  
 [12] L. A. Marqués, M. Aboy, M. Ruiz, I. Santos, P. López, L. Pelaz, "Molecular dynamics simulation of the early stages of self-interstitial clustering in silicon", *Mat. Sci. Semicon. Proc.* 42, 235 (2016)  
 [13] K. J. Dudeck, L. A. Marqués, A. P. Knights, R. M. Gwilliam, and G. A. Botton, "Sub-ångstrom Experimental Validation of Molecular Dynamics for Predictive Modeling of Extended Defect Structures in Si, *Phys. Rev. Lett.* 110, 166102 (2013)

